INTERNATIONAL JOURNAL FOR NUMERICAL METHODS IN FLUIDS
Int. J. Numer. Meth. Fluids **29**: 193–206 (1999)

NUMERICAL METHODS FOR THE SOLUTION OF THE TURBULENCE ENERGY EQUATIONS IN SHELF SEAS

J.D. ANNAN*

Proudman Oceanographic Laboratory, Bidston Observatory, Birkenhead, Merseyside L43 7RA, UK

SUMMARY

This paper investigates the accuracy of numerical finite difference methods for solving the turbulence kinetic energy equations in thermally stratified shelf seas with wind and tidal mixing. Alternative discretisation methods are presented for both the source terms and the diffusion term in the turbulence kinetic energy equation. It is shown that techniques not widely used in this field maintain greater accuracy at low spatial and temporal resolution than is obtained with commonly used ones, with no added computational cost. Therefore, these techniques are valuable for use in three-dimensional models.

KEY WORDS: finite difference; turbulence kinetic energy

1. INTRODUCTION

The development of thermal stratification in shallow seas is a complex process in which turbulent mixing (forced by the tide and wind) and surface heating and cooling of the ocean interact. Systems of physical equations of varying complexity can be constructed to describe these processes, and approximate solutions to these may be obtained via numerical models based on finite difference schemes. To facilitate the computation of solutions to the turbulence kinetic energy (TKE) equations, several different discretisation schemes have been proposed and tested in one-dimensional numerical models [1–3]. The accuracy of these schemes has usually been of secondary importance to numerical stability, since extremely high temporal and spatial resolution can easily be obtained for one-dimensional models with modern computing power. This is true even for the more complex schemes in widespread use in marine modelling (e.g. the Mellor–Yamada Level 2.5 scheme [2,4], or the k–ϵ model as described by Baumert and Radach [3]). For instance, Davies and Jones [1] used 100 irregularly spaced grid points in 10 m of water (with a grid size of 0.005 m in the near-bed region) and a time step of 0.05 s to generate results in the bottom boundary layer; Baumert and Radach [3] used 50 vertical levels for water depths of between 5 and 100 m with a 300 s time step.

In three-dimensional models, such high temporal and spatial resolution is not computationally feasible. Proctor and James [5] used only 10 vertical levels for their high (2.4 km horizontal) resolution model of the southern North Sea. The largest time step they could use to solve the baroclinic equations, without unacceptably degrading the solution, was 600 s.

* Correspondence to: Proudman Oceanographic Laboratory, Bidston Observatory, Birkenhead, Merseyside L43 7RA, UK; e-mail: jdan@pol.ac.uk

CCC 0271–2091/99/020193–14$17.50

Received November 1996
Revised September 1997

Even at such low vertical and temporal resolution, their model required 2 h of CPU time, on a single processor CRAY EL9O, for each model day. Pohlmann's model of the North Sea [6], with a much lower horizontal resolution of 20 km, used 20 vertical levels and a time step of 1350 s. Both of these models used simpler vertical mixing schemes than those contained in the one-dimensional studies referred to above. Proctor and James used a simple Richardson number-based scheme, and Pohlmann used an equilibrium version of the $k-\epsilon$ model, ignoring vertical advection and diffusion.

Warrach [7] compared different turbulence closure schemes in a one-dimensional model of the North Sea. From the schemes tested, Warrach found that a method used by Sharples and Simpson [8], a variant on the Mellor–Yamada Level 2.5 scheme [9], gave better results than simpler schemes, similar to those used in the three-dimensional models mentioned above. Warrach also found that a one-dimensional model was not capable of fully explaining the vertical temperature structure, since there is seasonally varying horizontal advection. Warrach's preferred turbulence closure scheme involved the solution of an unsteady vertical diffusion equation for TKE, and so is computationally more demanding than the simpler schemes tested.

Computational speed and numerical errors are therefore important factors in the accurate three-dimensional numerical modelling of shelf seas. The purpose of this paper is to investigate numerical techniques suitable for the accurate modelling of the TKE equations at low spatial and temporal resolution. Firstly, an approximately implicit discretisation of the source terms, based upon a tangential linearisation, is shown to decrease numerical error while maintaining stability for large time steps. Secondly, it is shown that where interpolation of diffusion coefficients is required, the use of the harmonic mean increases accuracy at low spatial resolution when compared with the more obvious arithmetic mean.

2. THE MODEL

The model used here is a one-dimensional vertical mixing model on a regular staggered grid, based on one described in some detail by Sharples and Tett [10] and modified by Warrach [7]. The water column is divided into N equally sized elements, with velocities and scalars calculated at the midpoint of each element, and turbulent variables calculated at interfaces between the elements. The original model was a coupled physical and biological model, which used the Mellor–Yamada Level 2 turbulence closure scheme [4,11]. Warrach concentrated on the physical submodel (as is done here) and implemented and compared three different turbulence schemes.

The model consists of equations for horizontal motion, heat flux and diffusion, the turbulence closure scheme and the equation of state. The equation of state is taken from Gill [12], with a constant salinity of 34.8 ppt.

The horizontal equations of motion are:

$$\frac{\partial u}{\partial t} = -A_x \sin(\omega t - \phi_x) + fv + \frac{\partial}{\partial z}\left(N_z \frac{\partial u}{\partial z}\right), \tag{1}$$

$$\frac{\partial v}{\partial t} = -A_y \sin(\omega t - \phi_y) - fu + \frac{\partial}{\partial z}\left(N_z \frac{\partial v}{\partial z}\right), \tag{2}$$

where u and v are the velocities in the x-direction (eastward) and in the y-direction (northward) respectively, f is the coriolis factor, A_x and A_y are the tidal surface slope

amplitudes (multiplied by g), ϕ_x and ϕ_y are the tidal slope phases and ω the tidal frequency. N_z is the vertical eddy viscosity.

A bottom boundary stress is applied to the bottom cell via

$$\tau_{bx} = -u_1 k_b \rho (u_1^2 + v_1^2)^{1/2} \tag{3}$$

and

$$\tau_{by} = -v_1 k_b \rho (u_1^2 + v_1^2)^{1/2}, \tag{4}$$

where u_1 and v_1 are the near-bed velocities in the x- and y-direction respectively, ρ is the water density and $k_b = 0.003$ is the friction coefficient.

Wind stress is applied to the surface element via

$$\tau_{sx} = -u_w k_s \rho_a (u_w^2 + v_w^2)^{1/2} \tag{5}$$

and

$$\tau_{sy} = -v_w k_s \rho_a (u_w^2 + v_w^2)^{1/2}, \tag{6}$$

where u_w and v_w are the x- and y-components of the wind velocities, ρ_a is the air density (1.2 kg m^{-3}) and $k_s = 0.0014$ is the surface drag coefficient.

The heat diffusion equation is

$$\frac{\partial T}{\partial t} = \frac{\partial}{\partial z}\left(K_z \frac{\partial T}{\partial z}\right), \tag{7}$$

where T is the temperature and K_z is the coefficient of vertical eddy diffusivity.

There is no heat flux through the sea bed, and surface heating follows the approach of Simpson and Bowers [13], which requires inputs of solar radiation J_s (W m^{-2}), dewpoint temperature T_d (°C) and wind speed w (m s^{-1}).

The net heat input is given by the following set of equations.

$$J = J_s + k(T_d - T_s), \tag{8}$$

with T_s being the surface temperature and

$$k = 4.5 + 0.05T_s + (\beta + 0.47)f(w), \tag{9}$$

$$\beta = 0.35 + 0.015T_m + 0.0012T_m^2, \tag{10}$$

$$T_m = 0.5(T_d + T_s), \tag{11}$$

$$f(w) = 9.2 + 0.46w^2. \tag{12}$$

The cooling term $k(T_d - T_s)$ is applied to the surface element and the solar radiation is distributed throughout the water column via

$$\frac{\partial J_s(z)}{\partial z} = -\lambda_0 J_s(z), \tag{13}$$

with $\lambda_0 = 0.154$ m^{-1} being the attenuation coefficient.

The TKE equation used by the Mellor–Yamada Level 2.5 model is given by

$$\frac{\partial Q}{\partial t} = \frac{\partial}{\partial z}\left(K_q \frac{\partial Q}{\partial z}\right) + N_z\left(\left(\frac{\partial u}{\partial z}\right)^2 + \left(\frac{\partial v}{\partial z}\right)^2\right) + K_z \frac{g}{\rho_0}\frac{\partial \rho}{\partial z} - \frac{q^3}{B_1 l}, \tag{14}$$

where $Q = q^2/2$ is the turbulent kinetic energy (q is the turbulent intensity), K_q is the coefficient of turbulent diffusivity, B_1 is an empirically determined constant (with the value 15.0), ρ_0 and ρ are the initial and present density respectively, and l is the turbulent lengthscale. Following Sharples and Simpson [8], the turbulent lengthscale l is given by

$$l = \kappa z \sqrt{1 - z/h}, \tag{15}$$

where $\kappa = 0.41$ is the von Karman constant, z is the distance above the seabed and h is the total water depth. The constraint

$$l \leq \sqrt{\frac{0.28q^2}{N^2}} \tag{16}$$

is also used, where $N^2 = -(g/\rho_0)(\partial\rho/\partial z)$ is the Brundt–Väisälä frequency.

The turbulent coefficients are calculated by

$$N_z = S_m l q, \tag{17}$$

$$K_z = S_h l q, \tag{18}$$

$$K_q = 0.2 l q. \tag{19}$$

The stability functions S_m, S_h in the above are given by

$$S_m = A_1 \frac{1 - 3C_1 - 6A_1/B_1 - 3A_2 G_h((B_2 - 3A_2)(1 - 6A_1/B_1) - 3C_1(B_2 + A_1))}{(1 - 3A_2 G_h(6A_1 + B_2))(1 - 9A_1 A_2 G_h)} \tag{20}$$

and

$$S_h = A_2 \frac{1 - 6A_1/B_1}{1 - 3A_2 G_h(6A_1 + B_2)}, \tag{21}$$

with

$$G_h = -\frac{l^2}{q^2} N^2 \tag{22}$$

subject to

$$-0.28 \leq G_h \leq 0.0233, \tag{23}$$

with the constants A_1, A_2, B_1, B_2, C_1 equal to 0.92, 0.74, 16.6, 10.1, 0.08 respectively [9].

There is a known deficiency of the above model in its behaviour where highly stably stratified conditions exist. In the absence of other constraints, the TKE can decrease to zero. An explanation for this physically unrealistic result, is that the model equations as given above do not take into account other sources of turbulence, such as the breaking of internal waves. This situation is prevented from occurring by imposing lower limits of 1.1×10^{-5} m^2 s^{-1} on the coefficients N_z, K_z and K_q, and a lower limit on the TKE of 10^{-12} m^2 s^{-2}.

The model described by Warrach used an explicit temporal discretisation for the diffusion terms in the heat, momentum and TKE equations. This limited the time step to 18 s to ensure numerical stability. In three-dimensional modelling, the baroclinic equations are commonly discretised in a partially implicit form in order to remove this limitation and so allow an increase in computational speed. In order to provide a valid comparison with the methods used in three-dimensional modelling, the diffusion terms have all been discretised in this manner in this study, as described in more detail below.

The discretised water column is divided up into N equally sized cells with the velocities and scalars calculated at the centre of each cell and indexed by $i = 1, \ldots, N$ (with i increasing from the seabed to the surface). The turbulent energy and associated diffusion coefficients are evaluated at the interfaces of the cells and indexed by $i = 3/2, 5/2, \ldots, (N-1)/2$. Using Q^{old} (Q^{new}) to indicate the value of Q before (after) a time interval Δt, the discretised TKE equation is written as:

$$\frac{Q^{\text{new}}_{i+1/2} - Q^{\text{old}}_{i+1/2}}{\Delta t} = \frac{(K_q)_{i+1}(Q^{\text{new}}_{i+3/2} - Q^{\text{new}}_{i+1/2}) - (K_q)_i(Q^{\text{new}}_{i+1/2} - Q^{\text{new}}_{i-1/2})}{(\Delta z)^2} + S_{\text{TKE}}(Q_{i+1/2}), \tag{24}$$

where the diffusion coefficients K_q are evaluated at the lower time level. The temporal discretisation of the source term $S_{\text{TKE}}(Q_{i+1/2})$ has deliberately been ambiguous as it will be considered in more detail later. It can also be seen from Equation (24) that the diffusion coefficients K_q are required at the scalar points in the grid, and so some form of interpolation is required. This is also considered in more detail in a later section.

The vertical diffusion of heat and momentum are discretised in a similar manner, i.e. for temperature,

$$\frac{T^{\text{new}}_i - T^{\text{old}}_i}{\Delta t} = \frac{(K_z)_{i+1/2}(T^{\text{new}}_{i+1} - T^{\text{new}}_i) - (K_z)_{i-1/2}(T^{\text{new}}_i - T^{\text{new}}_{i-1})}{(\Delta z)^2} + S^{\text{old}}_{\text{HEAT}}(T_i), \tag{25}$$

with K_z evaluated at the lower time level and the source term evaluated explicitly according to Equations (8)–(13). For velocity in the x-direction,

$$\frac{u^{\text{new}}_i - u^{\text{old}}_i}{\Delta t} = \frac{(N_z)_{i+1/2}(u^{\text{new}}_{i+1} - u^{\text{new}}_i) - (N_z)_{i-1/2}(u^{\text{new}}_i - u^{\text{new}}_{i-1})}{(\Delta z)^2} + S^{\text{old}}_{\text{MOM}}(u_i), \tag{26}$$

with the equation of motion in the y-direction analogous. The evaluation of the source term is again fully explicit. In principle, an explicit evaluation of the bottom friction term imposes a stability constraint on the time step, but in practice this constraint is so large so as not to matter (unless the water is extremely shallow).

A fully implicit discretisation, evaluating all the diffusion coefficients and the source terms in each equation at the higher time level, would computationally be more intensive, and is not usually performed. In the following sections accurate numerical methods for evaluating the terms in the TKE equation are investigated.

3. TEMPORAL DISCRETISATION OF SOURCE TERM

The source term is defined by the following:

$$S = N_z\left(\left(\frac{\partial u}{\partial z}\right)^2 + \left(\frac{\partial v}{\partial z}\right)^2\right) + K_z\frac{g}{\rho_0}\frac{\partial \rho}{\partial z} + \frac{-q^3}{B_1 l}. \tag{27}$$

The terms on the right-hand side represent shear production, work done against buoyancy and dissipation respectively. The shear production term is always positive, representing a source, and the dissipation term is always negative. The buoyancy term, which is usually negative (in stably stratified water), can briefly become positive when unstably stratified conditions are created.

Note that these three terms depend on the turbulent kinetic energy Q since the coefficients N_z and K_z are proportional to the turbulent intensity via (17)–(19). These terms can be written as:

$$N_z\left(\left(\frac{\partial u}{\partial z}\right)^2+\left(\frac{\partial v}{\partial z}\right)^2\right)=\alpha Q^{1/2}, \tag{28}$$

$$K_z\frac{g}{\rho_0}\frac{\partial \rho}{\partial z}=\beta Q^{1/2}, \tag{29}$$

$$\frac{-q^3}{B_1 l}=\gamma Q^{3/2}, \tag{30}$$

with appropriate choices for the functions α, β and γ. The functions α and β have a weak dependence on Q through the function G_H and the stability functions S_M and S_H (17)–(22). However, G_H is typically either at one of the limits of its range (Equation (23)) or else (in well-mixed water) it is very close to zero, and in these cases a change in TKE has a very small effect. Therefore, α, β and γ are treated as constants over a single time step in the above equations.

3.1. Methods

The simplest way of evaluating the source terms is to use a fully explicit approach: the previously calculated values of Q (and all other variables) associated with the lower time level are used in the finite difference calculation. This method, also known as the explicit Euler method, is unstable unless a very short time step is used ([14]; chapter 16). The large negative buoyancy term present in an area of stably stratified water can force the calculated value of Q at the next time level (which is written as Q^{new}) to become negative, unless an extremely short time step is used. This is of course undesirable since it is physically impossible. In practice, a lower bound is placed on the value of Q for reasons previously discussed, and the new value is corrected if necessary after calculation.

A method of removing this instability was suggested by Baumert and Radach [3]. In their formulation, a time-varying polynomial Q^n is evaluated by taking a single power of Q, evaluated at the higher time level, and all other powers of Q at the lower time level, i.e.:

$$Q^n = Q^{\text{new}}(Q^{\text{old}})^{n-1} \tag{31}$$

for any n. Using their method, one would write $Q^{3/2}=Q^{\text{new}}(Q^{\text{old}})^{1/2}$; and $Q^{1/2}=Q^{\text{new}}(Q^{\text{old}})^{-1/2}$. Making the first of these substitutions in the dissipation term, and the second substitution in the buoyancy term when it is negative, ensures that the TKE cannot overshoot zero however long the time step is. This method is only applied to negative source terms: if either the shear production term or the buoyancy term in unstably stratified conditions is treated in this manner, then a new instability may arise, for reasons which will be explained below.

Davies and Jones [1] compared different discretisations of the dissipation term, and preferred another method of evaluating this term over the Baumert and Radach approach. In the notation of this paper, they discretised $Q^{3/2}$ in the dissipation term as $2Q^{\text{new}}(Q^{\text{old}})^{1/2}-(Q^{\text{old}})^{3/2}$, and found that this was stable for time steps of up to 1490 s. The combination of the Davies and Jones' method for the dissipation term, plus the Baumert and Radach method for the buoyancy term, ensures stability and positive values for the TKE for an arbitrarily long time step. Although this method ensures stability, it does not necessarily ensure accuracy. Davies and Jones found that for a time step of 1490 s, their numerical error was unacceptably large.

When evaluating source terms, a time weighting term can be used to interpolate in the interval $(S(Q^{\text{old}}), S(Q^{\text{new}}))$. For a very short time step, the midpoint of the interval (Crank–Nicholson technique) is the most accurate choice, although in practice any intermediate value

will suffice since the interval is small. For a relatively long time step, however, an explicit scheme is numerically unstable and the Crank–Nicholson scheme will often generate spurious oscillations. Over a long time step, the TKE will approach a quasi-steady state, as is demonstrated by the reasonable success of the simpler equilibrium versions of the TKE equations. Therefore, an implicit scheme should give good results since the source term at the higher time level will predominate over the time step. There are many more complex methods that could in principle be used for integration of the source terms, such as the Runge–Kutta methods or Adams–Bashforth–Moulton schemes. However, in each case, the 'predictor' step is an explicit one, and unless a computationally intensive iterative scheme or an adaptive step size is implemented, these methods do not even guarantee stability. Implementing an implicit scheme exactly would also require massive computational effort, since an iterative approach would be needed. The best that can be achieved in a single computational step is to approximate the source terms with a linear function:

$$S(Q^{\text{new}}) \simeq b_0 + b_1 Q^{\text{new}}, \tag{32}$$

where b_0 and b_1 are constant for the duration of a time step.

For a general function $S = S(Q)$, the linear approximation to $S(Q^{\text{new}})$ is calculated by the first-order Taylor series, as suggested by Patankar [15]:

$$S(Q^{\text{new}}) \simeq S(Q^{\text{old}}) + \left.\frac{\partial S}{\partial Q}\right|_{Q^{\text{old}}} (Q^{\text{new}} - Q^{\text{old}}). \tag{33}$$

It is easy to see that the terms in this equation (which is called tangential linearisation) can be rearranged within a finite difference scheme for Q, since the dependance on Q^{new} is linear. This method is sometimes referred to as semi-implicit, since the linearisation is only an approximation to the fully implicit method, but it is preferable to avoid this expression as it is also sometimes used to refer to the time-centred method.

For the source terms, we have

$$\alpha(Q^{\text{new}})^{1/2} \simeq \frac{\alpha(Q^{\text{old}})^{1/2}}{2} + Q^{\text{new}} \frac{\alpha}{2(Q^{\text{old}})^{1/2}}, \tag{34}$$

$$\beta(Q^{\text{new}})^{1/2} \simeq \frac{\beta(Q^{\text{old}})^{1/2}}{2} + Q^{\text{new}} \frac{\beta}{2(Q^{\text{old}})^{1/2}}, \tag{35}$$

$$\gamma(Q^{\text{new}})^{3/2} \simeq -\frac{\gamma(Q^{\text{old}})^{3/2}}{2} + Q^{\text{new}} \frac{3\gamma(Q^{\text{old}})^{1/2}}{2}. \tag{36}$$

The other methods previously described can also be called linear approximations around the point $(Q^{\text{old}}, S(Q^{\text{old}}))$. For example, the explicit method gives $b_0 = S(Q^{\text{old}})$, $b_1 = 0$ in Equation (32) and the Baumert and Radach treatment of negative terms gives $b_0 = 0$ and $b_1 = S(Q^{\text{old}})/Q^{\text{old}}$.

There are two minor computational issues that must be considered when using any linear approximation. The first is that the coefficient of Q^{new} in (32) cannot be positive. This is the problem, mentioned earlier, that would arise if the Baumert and Radach method was used for discretising a positive buoyancy or shear production term. It could also arise from the Taylor series in unstably stratifed water. If this coefficient, given by the gradient $\partial S/\partial|_{Q^{\text{old}}}$ is positive, then a singularity arises and unrealistically large positive or negative solutions may result. This can be explained by considering the physical interpretation of the positive coefficient: it implies that for an increase in Q, the source will also increase. In reality, if the gradient of the source function is positive, it can only be so over a small interval, since the negative dissipation term

will dominate when Q grows very large, and all of the source terms vanish at $Q = 0$. When the gradient is positive, this instability is prevented by reverting to the explicit formulation, evaluating the source terms at Q^{old}. This is effectively forcing the gradient of the linear approximation to be zero, and is the smallest adjustment to the tangential linearisation that eliminates the unwanted positive feedback.

The second problem that must be avoided is that the constant term b_0 in (32) must be non-negative. A negative constant term would imply that the source is a sink, even when Q^{new} drops to zero and beyond. This can produce negative solutions to the discretised equations. This is the cause of the instability in the explicit formulation. The problem can be avoided by modifying the linear approximation. Instead of using the tangential linearisation, the source function is approximated by the line passing through the current $(Q^{\text{old}}, S(Q^{\text{old}}))$ position and the origin. This line is described by $b_0 = 0$, $b_1 = S(Q^{\text{old}})/Q^{\text{old}}$, and so is similar to the method described by Baumert and Radach (the difference being that all terms can be treated in this way, since the coefficient of Q^{new} will remain negative). This modification is the smallest modification to the Taylor series expansion that eliminates the problem of the negative constant term.

3.2. Results

Numerical experiments were performed in order to test the performance of different treatments of the source terms. Three different formulations were used; explicit source terms (abbreviated to EX), the combination of the Davies and Jones method for dissipation, with the Baumert and Radach method for the buoyancy term (abbreviated to DJBR), and the tangential linearisation technique (abbreviated to TL). The model was run for a period of 250 days starting from the 6th of March 1989, at the point 55° 30′ N, 00° 54′ E, where *in situ* temperature measurements had been taken as part of the North Sea Community Project [16]. The meteorological inputs come from local forecasts and measurements. The wind speed and direction were taken from the UK Meteorological Office model, on a 3-h basis, and then linearly interpolated to hourly values. Hourly solar radiation means were taken from Hemsby, the nearest coastal station to the modelled location. Dewpoint temperatures were available from Tynemouth at 3-h intervals, and again these values were interpolated to hourly values. The tidal forcing was provided by the M_2 amplitude and phase, obtained from the POL CSX model [17]. The results of each method are compared when run with different time steps. Throughout this experiment, 21 grid points were used, which corresponds to a vertical spacing of 4 m. Spatial discretisation error is considered later. At the smallest time step used, $\Delta t = 3.6$ s, all models were close to convergence. For such a short time step, double precision arithmetic was required in order to reduce round-off error to acceptable levels. Each model run produces daily temperature depth profiles over a 250 day interval (6 March to 11 November), which covers the onset of thermal stratification through to the erosion of the thermocline. To produce a simple scalar measure of the difference between two model runs, the root mean square (rms) of the differences between the corresponding temperature predictions for each grid point at each day, throughout the entire 250 day run, were computed. A comparison of model results is given in Table I. Figure 1 provides a visual comparison of modelled temperature profiles at 40-day intervals for some of the model runs.

The columns labelled EX, DJBR and TL correspond to the explicit, Davies–Jones–Baumert–Radach and tangential linearisation respectively. The top three rows of each column show the rms of differences between the outputs of the three different techniques when all are run at the shortest time step of $\Delta t = 3.6$ s. The lower rows show how, for each technique, the model output diverges from the high resolution run as the time step increases.

Table I. RMS of the differences (°C) between model outputs with different source term treatments and time steps, with respect to $\Delta t = 3.6$ s runs

	EX ($\Delta t = 3.6$s)	DJBR ($\Delta t = 3.6$s)	TL ($\Delta t = 3.6$s)
EX ($\Delta t = 3.6$ s)	0.0	0.022	0.014
DJBR ($\Delta t = 3.6$ s)	X	0.0	0.013
TL ($\Delta t = 3.6$ s)	X	X	0.0
$\Delta t = 18$ s	0.005	0.022	0.014
$\Delta t = 36$ s	0.009	0.056	0.015
$\Delta t = 180$ s	0.059	0.15	0.064
$\Delta t = 360$ s	0.064	0.23	0.058
$\Delta t = 720$ s	0.12	0.34	0.084
$\Delta t = 900$ s	0.15	0.43	0.11
$\Delta t = 1200$ s	0.28	0.48	0.28

3.3. Discussion

Table I shows that, at the smaller time steps, all three methods produced virtually identical temperature profiles. As the time step increases, the output from the DJBR method diverges more rapidly than that from the other methods, and the position of the thermocline, seen in Figure 1, can be up to 5 m too high for the 900 s run. The inaccuracy of the DJBR technique can be explained by considering how their treatment of the source term differs from the tangential liearisation. The DJBR-linearised approximation to the dissipation term is steeper than the tangent (by a factor of one third), and the linearised buoyancy term, in stably stratified water, is twice as steep as the tangent (as is shown by Equations (34)–(36)). Both of these conditions contribute to slowing the change in Q when there is a large net sink. This is effectively an underrelaxation, which has the beneficial consequence of preventing negative

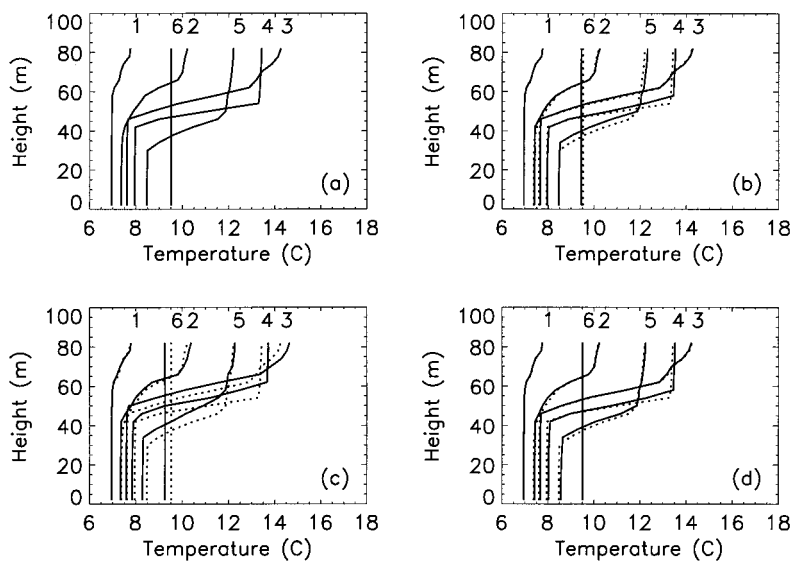

Figure 1. Solid lines show temperature (°C) at 40-day intervals (line 1 = 15 April, line 6 = 1 November) calculated for (a) $\Delta t = 3.6$ s; (b) $\Delta t = 900$ s, explicit method; (c) $\Delta t = 900$ s, DJBR method; and (d) $\Delta t = 900$ s, tangential linearisation. Dotted lines in (b)–(d) give results of (a) for comparison.

values, but also prevents Q from decaying as rapidly as the equations intend. The explicit treatment does not have this problem of underrelaxation, and gives more accurate results. It is interesting to note that the instability of the explicit technique does not appear to generate serious errors in the modelled temperature profile. However, the numerical instability generates non-physical oscillations in the TKE values, even at the lowest time step tested, and so the explicit formulation cannot be recommended for general use. The linearised method combines the strengths the other techniques without the drawbacks. It is as accurate as the explicit method for short time steps, and even reduces errors by around one third for typical time steps (for a three-dimensional model) of 720–900 s. This method is stable, and so avoids the problems of overshoot and non-physical negative energies. The errors arising from the linearised method are lower than those arising from the DJBR method for the same time step. The 900 s time step run using the tangential linearisation produces a more accurate output than the 180 s run of the DJRB technique. This is striking given that the only change between the models is the modification of one part of one of the model equations; whereas the measure of numerical error is the sum of all error sources. At larger time steps than those shown here, all the models produce poor outputs. This suggests that other numerical errors are starting to overwhelm the differences between the techniques.

4. SPATIAL DISCRETISATION OF DIFFUSION TERM

Now attention is turned to the interpolation of the diffusion coefficients in the TKE equation.

The discretised form of the equation requires values for K_q at the scalar grid points $i = 1, \ldots, N$. However, TKE (and therefore K_q) is calculated at the intermediate grid points, and so some form of interpolation is required between adjacent values. If the two adjacent values of K_q are similar, then the method of interpolation selected is not important, as they will all give similar results. However, in a model that includes thermal stratification, there is usually an extremely abrupt transition between a well-mixed area, where there is high TKE (and so K_q is also high), and a stably stratified thermocline, where there is a very low level of TKE (and so K_q is extremely low). Adjacent values of K_q can vary by as much as three orders of magnitude, even at high spatial resolution. These conditions present a severe test for a low resolution numerical model, and it is important that the interpolation is performed correctly in order that the diffusion of TKE may be modelled accurately.

Various interpolation procedures are considered, and the results obtained when the different methods are used in the numerical model are compared.

4.1. Methods

An obvious approach is simply to use the arithmetic mean,

$$(K_q)_i = \frac{(K_q)_{i-1/2} + (K_q)_{i+1/2}}{2}. \tag{37}$$

The mean gives a second-order approximation to the value of K_q at the midpoint. Davies and Jones use this form ([1]; equation 28]. Although many published descriptions of models do not contain such a detailed description of the discretised equations, it appears that this approach is widespread.

An accurate methodology for interpolation can be developed in the following way. The flux of TKE between the points $i - 1/2$ and $i + 1/2$ is discretised in Equation (24) as

$$K_q \frac{\partial Q}{\partial z} \simeq (K_q)_i \frac{Q_{i+1/2} - Q_{i-1/2}}{\Delta z}. \tag{38}$$

Calling the flux F, integration is performed in the following manner:

$$K_q \frac{\partial Q}{\partial z} = F, \tag{39}$$

$$\int_{i-1/2}^{i+1/2} \frac{\partial Q}{\partial z}\, \mathrm{d}z = \int_{1-1/2}^{i+1/2} \frac{F}{K_q(z)}\, \mathrm{d}z. \tag{40}$$

Taking F to be constant on $(i-1/2, i+1/2)$ one gets

$$Q_{i+1/2} - Q_{i-1/2} = F \int_{i-1/2}^{i+1/2} K_q(z)^{-1}\, \mathrm{d}z, \tag{41}$$

which is easily rearranged to give

$$\frac{\Delta z}{\displaystyle\int_{i-1/2}^{i+1/2} K_q(z)^{-1}\, \mathrm{d}z} \frac{Q_{i+1/2} - Q_{i-1/2}}{\Delta z} = F. \tag{42}$$

A comparison of Equation (42) with (38) indicates that $(K_q)_i$ should be defined:

$$(K_q)_i = \frac{\Delta z}{\displaystyle\int_{i-1/2}^{i+1/2} K_q(z)^{-1}\, \mathrm{d}z}. \tag{43}$$

Using this formula, and making an assumption about the variation of K_q over the interval, the interpolated value for $(K_q)_i$ can be calculated correctly. For instance, if the variation of K_q with z is linear, then the above expression yields

$$(K_q)_i = \frac{(K_q)_{i+1/2} - (K_q)_{i-1/2}}{\ln((K_q)_{i+1/2}) - \ln((K_q)_{i-1/2})} \tag{44}$$

(of course $(K_q)_i = (K_q)_{i+1/2} = (K_q)_{i-1/2}$ if the adjacent values are equal). Hereafter, this interpolation is referred to as the linear variation. This expression has been tested using the numerical experiments described in the following sections.

If the alternative assumption that the variation of Q is linear across the interval is made, then, since K_q varies with the square root of Q, one gets

$$(K_q)_i = \frac{(K_q)_{i+1/2} + (K_q)_{i-1/2}}{2}. \tag{45}$$

This gives precisely the arithmetic average that is commonly used.

An alternative assumption, suggested by Patankar [15], is that each calculated value of K_q at each grid point predominates over half of the region between the adjacent points, with an abrupt change in value where the regions meet. In this case, the appropriate interpolated value would be given by

$$(K_q)_i = \frac{2(K_q)_{i+1/2}(K_q)_{i-1/2}}{(K_q)_{i+1/2} + (K_q)_{i-1/2}}, \tag{46}$$

which is the harmonic mean of the two adjacent grid point values.

As a simple demonstration of the significance of the differences between the three interpolation methods given here, consider a case in which adjacent values of K_q vary by roughly two

Table II. RMS of the differences (°C) between model outputs with different interpolation techniques and spatial resolution, with respect to $\Delta z = 0.5$ s runs

	H ($\Delta z = 0.5$ s)	L ($\Delta z = 0.5$ s)	A ($\Delta z = 0.5$ s)
H ($\Delta z = 0.5$ s)	0.0	0.016	0.017
L ($\Delta z = 0.5$ s)	X	0.0	0.001
A ($\Delta z = 0.5$ s)	X	X	0.0
$\Delta z = 1$ m	0.20	0.23	0.23
$\Delta z = 2$ m	0.34	0.45	0.47
$\Delta z = 3$ m	0.39	0.57	0.60
$\Delta z = 4$ m	0.47	0.66	0.71
$\Delta z = 6$ m	0.47	0.72	0.85
$\Delta z = 12$ m	0.44	0.92	1.24

orders of magnitude, say $100(K_q)_{i+1/2} \simeq (K_q)_{i-1/2}$. In this case, the interpolated values for the simple average, linear variation and harmonic mean are, approximately, $50(K_q)_{i+1/2}$, $21(K_q)_{i+1/2}$ and $2(K_q)_{i+1/2}$ respectively. In the next section, how this difference affects the model output is investigated, and the method that gives the most accurate results is discovered.

4.2. Results

Numerical experiments similar to those in Section 3 were performed in order to compare the relative accuracies of the different schemes. The same numerical model and meteorological inputs were used as described previously. Each interpolation scheme was used at a variety of different spatial resolutions in order to show how the output diverged from the high resolution run as the grid spacing increased.

Each version of the model was run at resolutions ranging from 0.5 to 12 m (168 grid points and 7 grid points respectively). The rms of the differences between model runs were calculated as before, with the minor modification that in order to compare different spatial resolutions, the higher resolution temperature profiles were averaged to the lower resolution. A time step of 36 s was used in order to reduce temporal discretisation errors to a low level. This has already been shown to be more than adequate for the grid spacing of 4 m used in the previous set of experiments. In principle, the time step should be reduced as the spatial resolution increases, in order to ensure that temporal discretisation error remains small for runs with higher spatial resolution. This is due to the resolution of smaller spatial scales in the higher resolution models and the shorter diffusion time-scale between adjacent grid points. In practice, test runs with varying time steps demonstrated that the temporal truncation error is negligible by comparison with the spatial truncation error. The results are given in Table II, and Figure 2 provides a visual comparison of model outputs.

The columns labelled H, L and A correspond to harmonic interpolation, linear variation and the arithmetic mean respectively. The top three rows of each column show the rms of differences between outputs of the three different techniques when all are run at the highest resolution of $\Delta z = 0.5$ m. The lower rows show how, for each technique, the model output diverges from the high resolution run as the grid spacing increases.

4.3. Discussion

The data in Table II indicate that none of the models have completely converged, even at the highest spatial resolution used. There is a clear trend in the results for the total thermal

diffusion through the thermocline to decrease as the model resolution increases, resulting in cooler lower ocean layers. Even at the highest resolution runs, the grid spacing is insufficient to accurately model the extremely sharp gradients present at the upper and lower edges of the thermocline. However, at high resolution, the different models all produce essentially the same results. At low resolution, use of the harmonic mean results in a much lower numerical error than the other two methods tried. At 6 and 12 m vertical resolution, the numerical error for the harmonic mean is roughly one half and one third, respectively, of that produced by the arithmetic average. These runs are typical of the vertical resolution commonly obtained in three-dimensional numerical models [5,6]. A comparison of lines 4 and 5 (13 August and 22 September) in the four graphs of Figure 2 show that the thermocline is very weak in the low resolution runs except when harmonic interpolation is used. The inferior interpolation techniques allow much larger amounts of TKE to diffuse into the thermocline, thereby weakening it and also leading to increased thermal diffusion into the lower ocean layers.

5. CONCLUSIONS

Some modifications to commonly used techniques in numerical modelling of TKE have been presented and tested. These have the effect of increasing accuracy when used for large time steps and grid spacing. The tangential linearisation of the source terms maintains the stability over long time steps, which is a useful feature of the DJBR scheme, whilst greatly improving accuracy, producing a lower numerical error for a 900 s time step than the DJBR method produces with a 180 s time step. The explicit formulation appears to produce a satisfactory temperature profile, but is computationally unstable and generates spurious oscillations in the TKE, even at the lowest time step tested.

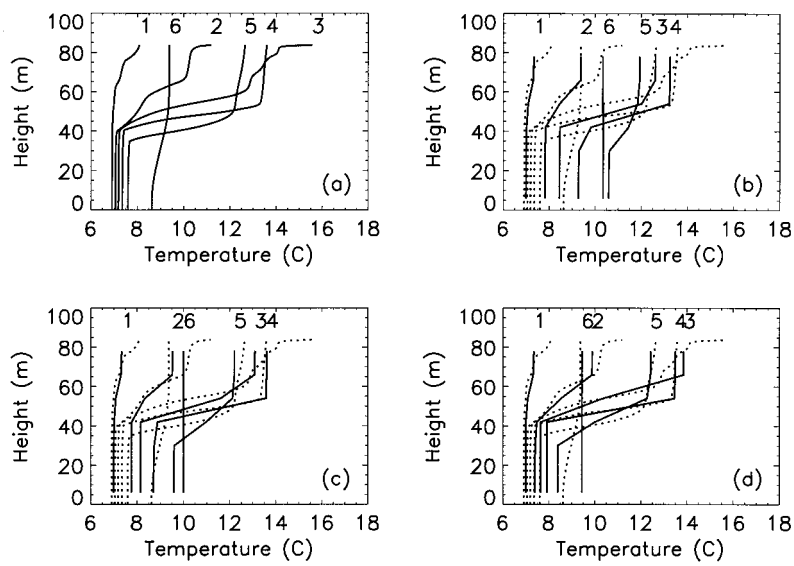

Figure 2. Solid lines show temperature (°C) at 40-day intervals (line 1 = 15 April, line 6 = 1 November) calculated for (a) $\Delta z = 0.5$ m; (b) $\Delta z = 12$ m, average interpolation; (c) $\Delta z = 12$ m, linear variation; and (d) $\Delta z = 12$ m, harmonic interpolation. Dotted lines in (b)–(d) give results of (a) for comparison.

Using the harmonic mean for the interpolation of diffusion coefficients leads to far greater accuracy at low spatial resolution, when compared with two other methods. The discretisation error is reduced to around one half or one third that arising from the use of the arithmetic average, when resolutions typical of three-dimensional models are used.

ACKNOWLEDGMENTS

This work was jointly funded by NERC and the UK Meteorological Office. The author would also like to thank J.C. Hargreaves and an anonymous referee for helpful comments and suggestions.

REFERENCES

1. A.M. Davies and J.E. Jones, 'On the numerical solution of the turbulence energy equations for wave and tide flow', *Int. J. Numer. Methods Fluids*, **12**, 17–41 (1991).
2. E. Deleersnijder and P. Luyten, 'On the practical advantages of the quasi-equilibrium version of the Mellor and Yamada level 2.5 turbulence closure applied to marine modeling', *Appl. Math. Model.*, **18**, 281–287 (1994).
3. H. Baumert and G. Radach, 'Hysteresis of turbulent kinetic energy in non-rotational tidal flows: a model study', *J. Geophys. Res.*, **97**, 3669–3677 (1992).
4. G.L. Mellor and T. Yamada, 'A hierarchy of turbulence closure models for planetary boundary layers', *J. Atmos. Sci.*, **31**, 1791–1806 (1974).
5. R. Proctor and I.D. James, 'A fine resolution 3D model of the southern North Sea', *J. Mar. Sys.*, **8**, 285–295 (1996).
6. T. Pohlmann, 'Predicting the thermocline in a circulation model of the North Sea—Part I: model description, calibration and verification', *Cont. Shelf Res.*, **16**, 168–194 (1996).
7. K.I. Warrach, 'Modelling the thermal stratification in the north sea', *J. Mar. Sys.*, **14**, 151–166 (1998).
8. J. Sharples and J.H. Simpson, 'Semi-diurnal and longer period stability cycles in the Liverpool Bay region of freshwater influence', *Cont. Shelf Res.*, **15**, 295–313 (1995).
9. B. Galperin, L.H. Kantha, S. Hassid and A. Rosati, 'A quasi-equilibrium turbulent energy model for geophysical flows', *J. Atmos. Sci.*, **45**, 55–62 (1988).
10. J. Sharples and P. Tett, 'Modelling the effect of physical variability on the midwater chlorophyll maximum', *J. Mar. Res.*, **52**, 219–238 (1994).
11. G.L. Mellor and T. Yamada, 'Development of a turbulence closure model for geophysical fluid problems', *Rev. Geophys. Space Phys.*, **20**, 851–875 (1982).
12. A.E. Gill, *Atmosphere—Ocean Dynamics*, Academic Press, New York, 1982.
13. J.H. Simpson and D.G. Bowers, 'The role of tidal stirring in controlling the seasonal heat cycle in shelf seas', *Ann. Geophys.*, **2**, 411–416 (1984).
14. W.H. Press, S.A. Teukolsky, W.T. Vetterling and B.P. Flannery, *Numerical Recipes in Fortran: The Art of Scientific Computing*, Cambridge University Press, Cambridge, MA, 1994.
15. S.V. Patankar, *Numerical Heat Transfer and Fluid Flow*, Hemisphere Publishing, Washinton, DC, 1980.
16. H. Charnock, K.R. Dyer, J.M. Huthnance, P.S. Liss, J.H. Simpson and P.B. Tett, *Understanding the North Sea System*, Royal Society, London, 1994.
17. R. Proctor and R.A. Flather, 'Routine storm forecasting using numerical models: procedures and computer programs for use on the CDC CYBER 205E at the British Meteorological Office'. *Technical Report 167*, Institute of Oceanographic Sciences, 1983.

